



This discussion paper is/has been under review for the journal Geoscientific Model Development (GMD). Please refer to the corresponding final paper in GMD if available.

# Simulation of polar stratospheric clouds in the chemistry-climate-model EMAC via the submodel PSC

O. Kirner<sup>1</sup>, R. Ruhnke<sup>2</sup>, J. Buchholz-Dietsch<sup>4</sup>, P. Jöckel<sup>3</sup>, C. Brühl<sup>4</sup>, and B. Steil<sup>4</sup>

<sup>1</sup>Karlsruhe Institute of Technology, Steinbuch Centre for Computing (SCC), Karlsruhe, Germany

<sup>2</sup>Karlsruhe Institute of Technology, Institute for Meteorology and Climate Research (IMK), Karlsruhe, Germany

<sup>3</sup>Deutsches Zentrum für Luft- u. Raumfahrt (DLR), Institut für Physik der Atmosphäre, Oberpfaffenhofen, Weßling, Germany

<sup>4</sup>Max Planck Institute for Chemistry (MPIC), Mainz, Germany

Received: 17 September 2010 – Accepted: 5 October 2010 – Published: 4 November 2010

Correspondence to: O. Kirner (ole.kirner@kit.edu)

Published by Copernicus Publications on behalf of the European Geosciences Union.

**GMDD**

3, 2071–2108, 2010

**The submodel PSC  
in EMAC**

O. Kirner et al.

Title Page

Abstract

Introduction

Conclusions

References

Tables

Figures

◀

▶

◀

▶

Back

Close

Full Screen / Esc

Printer-friendly Version

Interactive Discussion



## Abstract

The submodel PSC of the ECHAM5/MESy Atmospheric Chemistry model (EMAC) has been developed to simulate the main types of polar stratospheric clouds (PSC). The parameterisation of the supercooled ternary solutions (STS, type 1b PSC) in the submodel is based on Carslaw et al. (1995b), the thermodynamical approach to simulate ice particles (type 2 PSC) on Marti and Mauersberger (1993). For the formation of nitric acid trihydrate (NAT) particles (type 1a PSC) two different parameterisations exist. The first one is based on an instantaneous thermodynamical approach from Hanson and Mauersberger (1988), the second one (new implemented by Kirner, 2008) considers the growth of the NAT particles with aid of a surface growth factor based on Carslaw et al. (2002). Via namelist switches the NAT parameterisation, as well as some parameters for the NAT and ice formation can be chosen. This publication explains the background of the submodel PSC and the use of the submodel with the goal to simulate realistic PSC in EMAC.

## 1 Introduction

Polar stratospheric clouds are necessary for the understanding of the ozone depletion in polar spring. On the one hand the activation of inorganic chlorine and bromine substances takes place on their surfaces during the polar winter leading to ozone depletion in polar spring, on the other hand the denitrification of nitrogen substances and the dehydration of water vapour ( $\text{H}_2\text{O}$ ) is caused through the sedimentation of NAT and ice particles. The denitrification prevents the deactivation of the active halogen substances and the ozone depletion lasts longer.

PSC are classified into three subtypes. The type 1a PSC defined as solid NAT particles, the type 1b PSC as liquid STS droplets and solid ice particles form the type 2 PSC.

**GMDD**

3, 2071–2108, 2010

## The submodel PSC in EMAC

O. Kirner et al.

Title Page

Abstract

Introduction

Conclusions

References

Tables

Figures

⏪

⏩

◀

▶

Back

Close

Full Screen / Esc

Printer-friendly Version

Interactive Discussion



The exact microphysical and thermodynamical details of PSC development are still matter of discussion, but profound suggestions of their formation and existence in the polar atmosphere exist, which will be summarised briefly (Lowe and MacKenzie, 2008).

### 1.1 The formation of STS (type 1b PSC)

The formation of STS droplets ( $\text{HNO}_3 \cdot \text{H}_2\text{SO}_4 \cdot \text{H}_2\text{O}$ ) is described in Beyer et al. (1994), Carslaw et al. (1994, 1997) or Luo et al. (1995). STS form during cooling below a specific temperature threshold through uptake of nitric acid ( $\text{HNO}_3$ ) by sulphuric acid aerosols ( $\text{H}_2\text{SO}_4 \cdot \text{H}_2\text{O}$ ), existing in the so-called “Junge Layer” (Junge et al., 1961).

The ternary droplet composition depends on the temperature. In different laboratory measurements it has been shown that during cooling the fraction of  $\text{HNO}_3$  increases in the droplets, whereas the fraction of  $\text{H}_2\text{SO}_4$  decreases (Tabazadeh et al., 1994; Carslaw et al., 1995a; Luo et al., 1995; Beyer et al., 1994) forming STS. After Carslaw et al. (1994, 1997) the STS droplets are stable until the temperature drops to the ice frost point. With the uptake of  $\text{HNO}_3$  into the droplets also the volume of the STS particles is strongly increasing.

Besides the solubility of  $\text{HNO}_3$ , also the solubilities of hydrochloric acid (HCl), hypochlorous acid (HOCl), hydrobromic acid (HBr) and hypobromous acid (HOBr) are changing during cooling (Carslaw et al., 1997), which is important for the heterogeneous chemistry reactions (see Sect. 1.4).

### 1.2 The formation of NAT (type 1a PSC)

Mainly two assumptions for the formation of NAT particles ( $\text{HNO}_3 \cdot (\text{H}_2\text{O})_3$ ) exist: (1) the heterogeneous formation of NAT on ice particles (Biermann et al., 1998; Carslaw et al., 1998; Middlebrook et al., 1996; Waibel et al., 1999; Wirth et al., 1999) and (2) the homogeneous nucleation of NAT out of supercooled ternary solutions (Carslaw et al., 2002; Daerden et al., 2007; Tabazadeh et al., 2002).

## The submodel PSC in EMAC

O. Kirner et al.

Title Page

Abstract

Introduction

Conclusions

References

Tables

Figures

◀

▶

◀

▶

Back

Close

Full Screen / Esc

Printer-friendly Version

Interactive Discussion



As found by Hanson and Mauersberger (1988) NAT can exist under stratospheric conditions below the NAT condensation temperature ( $T_{\text{NAT}}$ ).  $T_{\text{NAT}}$  depends on the pressure and on the partial pressures of  $\text{HNO}_3$  and  $\text{H}_2\text{O}$ . A typical temperature for  $T_{\text{NAT}}$  is approx. 193 K. However observations (Schlager and Arnold, 1990; Dye et al., 1992) indicate that NAT particles do not exist before a supercooling of 2–3 K below  $T_{\text{NAT}}$ .

Former laboratory studies (Middlebrook et al., 1996; Biermann et al., 1998) and lidar observations on aircraft (Carslaw et al., 1998; Wirth et al., 1999) verify the first formation mechanism for NAT, the heterogeneous formation on ice particles. In this case  $\text{HNO}_3$  is adsorbed on ice particles, for instance if ice particles sediment through air with high  $\text{HNO}_3$  mixing ratios (Wofsy et al., 1990).

The second formation mechanism for NAT is the homogeneous nucleation of nitric acid dihydrate ( $\text{NAD}$ ,  $\text{HNO}_3 \cdot (\text{H}_2\text{O})_2$ ) out of STS and the subsequent conversion of the metastable NAD to NAT (Carslaw et al., 2002; Daerden et al., 2007). The NAD condensation temperature ( $T_{\text{NAD}}$ ) is approx. 2–3 K below  $T_{\text{NAT}}$  and it is possible to explain the observations of Schlager and Arnold (1990) and Dye et al. (1992). This formation mechanism is verified through labor studies from Tabazadeh et al. (2002).

### 1.3 The formation of ice (type 2 PSC)

Ice particles are formed in the stratosphere at very low temperatures, typically below the ice frost point ( $T_{\text{ice}}$ ) with approx. 188 K.

There are different processes forming ice. It has been debated which of them occur in the polar stratosphere: (1) homogeneous nucleation of ice out of supercooled sulphuric acid ( $\text{SSA}$ ,  $\text{H}_2\text{SO}_4 \cdot \text{H}_2\text{O}$ , Bertram et al., 1996) or out of supercooled ternary solutions (STS, Carslaw et al., 1998; Koop et al., 2000; Tabazadeh et al., 1997); (2) heterogeneous nucleation of ice out of liquid aerosol ( $\text{SSA}$ , STS) containing insoluble nuclei such as mineral oxides or soot (DeMott et al., 1997; Jensen and Toon, 1997); and (3) heterogeneous nucleation of ice on sulphuric acid tetrahydrate ( $\text{SAT}$ ,  $\text{H}_2\text{SO}_4 \cdot (\text{H}_2\text{O})_4$ , Fortin et al., 2003).

## The submodel PSC in EMAC

O. Kirner et al.

Title Page

Abstract

Introduction

Conclusions

References

Tables

Figures

◀

▶

◀

▶

Back

Close

Full Screen / Esc

Printer-friendly Version

Interactive Discussion



## The submodel PSC in EMAC

O. Kirner et al.

Title Page

Abstract

Introduction

Conclusions

References

Tables

Figures

◀

▶

◀

▶

Back

Close

Full Screen / Esc

Printer-friendly Version

Interactive Discussion



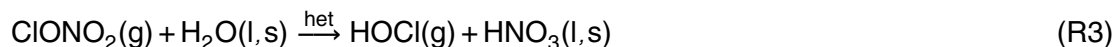
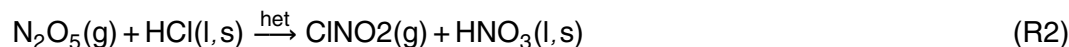
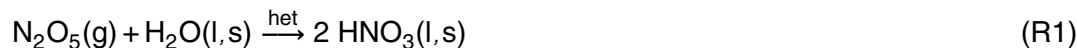
The first formation mechanism, the homogeneous nucleation of ice out of SSA or SST, is confirmed by different laboratory studies. This formation, however, requires a supercooling of some Kelvin. Tabazadeh et al. (1997) measured a supercooling of 2 to 3 K, Carslaw et al. (1998) of approx. 4 K and Daerden et al. (2007, deduced from Koop et al., 2000) of 3 to 4 K compared to the ice frost point.

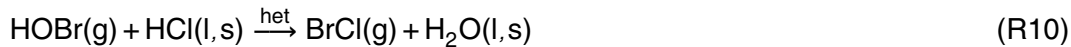
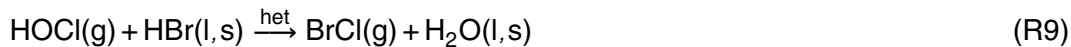
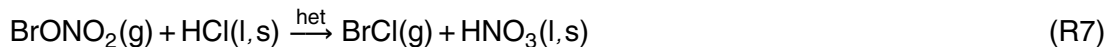
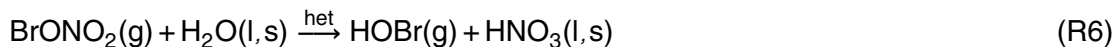
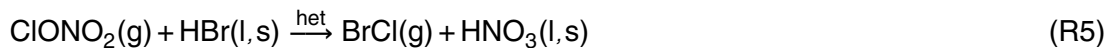
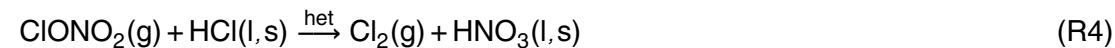
In contrast, theoretical work suggests that the second formation mechanism, the heterogeneous nucleation of ice out of SSA or STS with mineral oxide or soot as nuclei, may occur at temperatures warmer than those required for homogeneous nucleation (DeMott et al., 1997; Jensen and Toon, 1997). This mechanism is perhaps possible for the upper troposphere, where these nuclei exist, but improbable for the stratosphere (Fortin et al., 2003).

The third formation mechanism of ice particles, the deposition from water vapour on firm SAT particles introduced in Fortin et al. (2003) is most likely very relevant in the polar stratospheric atmosphere. It takes place at temperatures close to the ice frost point. In the laboratory studies of Fortin et al. (2003) only a supercooling of 0.1 K to 1.3 K was necessary for the formation.

### 1.4 Polar ozone depletion

PSCs are fundamental for the understanding of ozone depletion in polar spring. On the surfaces of the liquid and solid PSC particles the following heterogeneous reactions occur (Abbatt and Molina, 1992; Crutzen et al., 1992; Hanson and Ravishankara, 1991, 1993; Solomon et al., 1986; Tolbert et al., 1987):



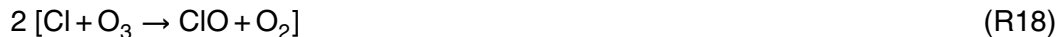


The products of these reactions: molecular chlorine ( $\text{Cl}_2$ ), molecular bromine ( $\text{Br}_2$ ), HOCl, HOBr, nitryl chloride (ClNO<sub>2</sub>) and bromine chloride (BrCl) are in gas phase (g); HNO<sub>3</sub> and H<sub>2</sub>O are in liquid (l) or solid phase (s).

During polar spring the gas phase products photolyse and ozone depleting radicals are formed (Reactions R12–R17):



The radicals deplete ozone in catalytic cycles. One example of such a catalytic cycle is the ozone depletion with Cl after Molina and Molina (1987):

**The submodel PSC  
in EMAC**

O. Kirner et al.

Title Page

Abstract

Introduction

Conclusions

References

Tables

Figures

◀

▶

◀

▶

Back

Close

Full Screen / Esc

Printer-friendly Version

Interactive Discussion





The self-reaction of the chlorine monoxide radicals (ClO) form chlorine monoxide dimer (Cl<sub>2</sub>O<sub>2</sub>) in this cycle.

Through the heterogeneous reactions on the surface of PSC particles and the subsequent photolysis in polar spring it is possible to explain the polar ozone depletion quantitatively (Graedel and Crutzen, 1993).

## 2 The EMAC model

The Chemistry Climate Model (CCM) EMAC (ECHAM5/MESSy Atmospheric Chemistry model; Jöckel et al. (2006)) has been developed at the Max-Planck-Institute for Chemistry in Mainz. EMAC is a combination of the general circulation model ECHAM5 (Roeckner et al., 2006) and different submodels as for instance the chemistry submodel MECCA1 (Sander et al., 2005) combined through the Modular Earth Submodel System (MESSy, Jöckel et al. (2005)).

In the vertical EMAC simulates (in a middle atmosphere setup) the atmosphere from the ground to 0.01 hPa (approx. 80 km), i.e., including the troposphere, stratosphere and mesosphere. Data are exchanged between the base model (ECHAM5) and the submodels within one comprehensive model system. With the generalized interface structure MESSy the standardized control of the submodels and their interconnections is possible.

Besides the submodel PSC for the simulation of polar stratospheric clouds and MECCA1 for the gas-phase chemistry the following submodels (among others) exist: OFFLEM for offline emissions of trace gases and aerosols (Kerkweg et al., 2006b), TNUDGE for tracer nudging (Kerkweg et al., 2006b), DRYDEP for dry deposition of trace gases and aerosols (Kerkweg et al., 2006a), SEDI for the sedimentation of

## The submodel PSC in EMAC

O. Kirner et al.

[Title Page](#)

[Abstract](#)

[Introduction](#)

[Conclusions](#)

[References](#)

[Tables](#)

[Figures](#)

[I◀](#)

[▶I](#)

[◀](#)

[▶](#)

[Back](#)

[Close](#)

[Full Screen / Esc](#)

[Printer-friendly Version](#)

[Interactive Discussion](#)



aerosol particles (Kerkweg et al., 2006a), JVAL for the calculation of photolysis rates (Landgraf and Crutzen, 1998), SCAV for the scavenging and liquid phase chemistry in cloud and precipitation (Tost et al., 2006a), CONVECT for the parameterization of convection (Tost et al., 2006b), LNOX for the source of NO<sub>x</sub> produced by lightning (Tost et al., 2007b), PTRAC for additional prognostic tracers (Jöckel et al., 2008), CVTRANS for convective tracer transport, TROPOP for diagnosing the tropopause and boundary layer height, H<sub>2</sub>O for stratospheric water vapour, RAD4ALL for the radiation calculation, HETCHEM for calculating reaction coefficients of heterogeneous reactions on aerosols (see Jöckel et al., 2006 and references therein), and CLOUD for calculating the cloud cover as well as cloud microphysics including precipitation (Tost et al., 2007a).

### 3 The submodel PSC

The submodel PSC is based on the “Mainz Photochemical Box Model” (Crutzen et al., 1992; Grooß, 1996; Meilinger, 2000; Müller, 1994) and was improved amongst others by Buchholz (2005) and Kirner (2008). The new version of this submodel, described in this publication, is available since EMAC version 1.9. It includes the simulation of the different PSC types. In the submodel parameterisations for the formation of STS droplets, the formation of NAT particles and the formation of ice particles exist. Moreover, it describes the sedimentation of these particles and the calculation of the heterogeneous chemistry reaction rate coefficients, which take place on the surface of the PSC particles. A new parameterisation for NAT particles based on the efficient growth and sedimentation algorithm of van den Broek et al. (2004) and Carslaw et al. (2002) has been implemented in the submodel by Kirner (2008).

#### 3.1 The parameterisation of STS droplets and stratospheric liquid aerosols

The calculation of STS droplets (type 1b PSC) is implemented in the calculation of stratospheric liquid aerosol and based on Carslaw et al. (1995b). With the aid of several

## The submodel PSC in EMAC

O. Kirner et al.

[Title Page](#)

[Abstract](#)

[Introduction](#)

[Conclusions](#)

[References](#)

[Tables](#)

[Figures](#)

[◀](#)

[▶](#)

[◀](#)

[▶](#)

[Back](#)

[Close](#)

[Full Screen / Esc](#)

[Printer-friendly Version](#)

[Interactive Discussion](#)



parameterisations the fractions of  $\text{H}_2\text{SO}_4$ ,  $\text{HNO}_3$ ,  $\text{H}_2\text{O}$ , as well as  $\text{HCl}$ ,  $\text{HOCl}$ ,  $\text{HBr}$  and  $\text{HOBr}$  in SSA and STS are calculated.

These parameterisations from Carslaw et al. (1995b) are valid for the temperature range  $185\text{ K} \leq T \leq 240\text{ K}$ .

The first step is the computation of the molar fractions (in  $\text{mol kg}^{-1}$ ) of  $\text{H}_2\text{SO}_4$  ( $b\text{H}_2\text{SO}_4(\text{binary})$ ) and  $\text{HNO}_3$  ( $b\text{HNO}_3(\text{binary})$ ) in the supercooled binary solutions ( $\text{H}_2\text{SO}_4 \cdot \text{H}_2\text{O}$  (SSA) and  $\text{HNO}_3 \cdot \text{H}_2\text{O}$ ). Thereby each fraction depends on pressure, temperature and on the mixing ratio of  $\text{H}_2\text{O}$ . At temperatures above 215 K the liquid fraction of  $\text{HNO}_3$  is set to zero.

In the second step the liquid molar fractions of  $\text{H}_2\text{SO}_4$  ( $b\text{H}_2\text{SO}_4(\text{ternary})$ ) and  $\text{HNO}_3$  ( $b\text{HNO}_3(\text{ternary})$ ) in the droplets are calculated. At temperatures above 215 K the  $b\text{HNO}_3(\text{ternary})$  is set to zero. After these calculations the mass fractions (in  $\text{kg kg}^{-1}$ ) of  $\text{H}_2\text{SO}_4$  ( $w\text{H}_2\text{SO}_4$ ) and  $\text{HNO}_3$  ( $w\text{HNO}_3$ ) in the liquid stratospheric aerosol are simulated (Carslaw et al., 1995b).

With the aid of the Henry coefficients ( $k_H$  in  $\text{mol kg}^{-1} \text{ mol}^{-1}$ , which mainly depend on the composition of the liquid aerosol, see Carslaw et al., 1997), the solubilities of  $\text{HCl}$ ,  $\text{HBr}$  (parameterisation from Luo et al., 1995),  $\text{HOCl}$  (Huthwelker et al., 1995) and  $\text{HOBr}$  (Hanson and Ravishankara, 1995) are calculated. With these solubilities it is possible to calculate the mass fractions of  $\text{HCl}$  ( $w\text{HCl}$ ),  $\text{HBr}$  ( $w\text{HBr}$ ),  $\text{HOCl}$  ( $w\text{HOCl}$ ),  $\text{HOBr}$  ( $w\text{HOBr}$ ) (in  $\text{kg kg}^{-1}$ ) in the liquid stratospheric aerosol. The mass fraction of  $\text{H}_2\text{O}$  is the difference of 1.0 to the calculated mass fractions.

The third step is the calculation of the mixing ratios of the substances which are in liquid phase ( $\text{H}_2\text{SO}_4(\text{liq})$ ,  $\text{HNO}_3(\text{liq})$ ,  $\text{H}_2\text{O}(\text{liq})$ ,  $\text{HCl}(\text{liq})$ ,  $\text{HBr}(\text{liq})$ ,  $\text{HOCl}(\text{liq})$ ,  $\text{HOBr}(\text{liq})$  in  $\text{mol mol}^{-1}$ ). It is assumed that the  $\text{H}_2\text{SO}_4$  is in the liquid phase in the stratosphere ( $\text{H}_2\text{SO}_4(\text{liq})$ ). The mixing ratios of the other liquid substances are calculated according to  $\text{H}_2\text{SO}_4(\text{liq})$ .

## The submodel PSC in EMAC

O. Kirner et al.

Title Page

Abstract

Introduction

Conclusions

References

Tables

Figures

⏪

⏩

◀

▶

Back

Close

Full Screen / Esc

Printer-friendly Version

Interactive Discussion



For example  $\text{H}_2\text{O}(\text{liq})$  is calculated through:

$$\text{H}_2\text{O}(\text{liq}) = \frac{w_{\text{H}_2\text{O}} \cdot \text{H}_2\text{SO}_4(\text{liq}) \cdot M_{\text{H}_2\text{O}}}{w_{\text{H}_2\text{SO}_4} \cdot M_{\text{H}_2\text{SO}_4}} \quad (1)$$

with  $M_{\text{H}_2\text{O}}$  and  $M_{\text{H}_2\text{SO}_4}$  being the molar masses of  $\text{H}_2\text{O}$  and  $\text{H}_2\text{SO}_4$ , respectively.

### 3.2 The parameterisation of NAT particles

5 For the formation of NAT particles (type 1a PSC) two different parameterisations exist. The first one is based on an instantaneous thermodynamical approach from Hanson and Mauersberger (1988) and is called in the following as “thermodynamical NAT parameterisation”. The second one considers the growth of the NAT particles with the aid of a surface growth factor based on Carslaw et al. (2002) and is called in the following as “kinetic growth NAT parameterisation”. The thermodynamical NAT parameterisation has been implemented in EMAC by Buchholz (2005), the kinetic growth parameterisation by Kirner (2008).

#### 3.2.1 Thermodynamical NAT parameterisation

15 The formation of solid PSC particles using the thermodynamical NAT parameterisation is based on the assumption that NAT only forms via heterogeneous formation of NAT on ice particles (see Sect. 1.2) and ice forms at supersaturation (see Sect. 1.3). For this approach a so called “phase concept” in the submodel PSC exists.

The formation of PSC particles is controlled through the model variable *phase*. It describes if the formation conditions of STS, NAT and ice exist or not:

- 20 – phase = 0 → no formation conditions for PSC,
- phase = 1 → formation conditions for STS,
- phase = 2 → formation conditions for STS and NAT,
- phase = 3 → formation conditions for STS, NAT and ice.

Outside a defined PSC region the variable *phase* is 0, within this region *phase* is always 1, 2 or 3, i.e., only in this region it is possible to form PSC. The boundaries (latitude, lower and upper limits) of the PSC region can be determined via the PSC submodel namelists (see Sect. 4).

The heterogeneous NAT formation on ice particles is the underlying assumption for the phase concept (Carslaw et al., 1998). If the temperature drops below  $T_{\text{ice}}$ , ice particles are formed and it is also possible to form NAT. The variable *phase* will be set to 3, if the total partial pressure of  $\text{H}_2\text{O}$  ( $e_{\text{H}_2\text{O}(\text{total})}$  in Pa, the sum of gas, liquid and solid  $\text{H}_2\text{O}$ ) is smaller than the saturation vapour pressure of  $\text{H}_2\text{O}$  over ice ( $E_{\text{H}_2\text{O}}^{\text{ice}}$  in Pa, calculated according to Marti and Mauersberger, 1993).

After melting of ice, the NAT existence is further possible as long as the conditions for NAT formation are given ( $T \leq T_{\text{NAT}}$ ). The variable *phase* will be set to 2, if the total partial pressure of  $\text{HNO}_3$  ( $e_{\text{HNO}_3(\text{total})}$  in Pa, the sum of gas, liquid and solid  $\text{HNO}_3$ ) is smaller than the saturation vapour pressure of  $\text{HNO}_3$  over NAT ( $E_{\text{HNO}_3}^{\text{NAT}}$  in Pa, calculated according to Hanson and Mauersberger, 1988).

Using the thermodynamical NAT parameterisation the homogeneous NAT formation (see Sect. 1.2) is only possible if the parameter *LHomNucNAT* from the PSC submodel namelists is set to *.TRUE.* (see Sect. 4). With the default setup it is not possible to change *phase* from 1 to 2.

With the help of the PSC submodel namelists, it is also possible to set supersaturations for ice and NAT formation (see Sect. 4).

With the aid of  $e_{\text{HNO}_3(\text{total})}$  and  $E_{\text{HNO}_3}^{\text{NAT}}$ , depending on temperature and on the mixing ratio of  $\text{HNO}_3$ , it is possible to simulate the mixing ratio of  $\text{HNO}_3$  contained in NAT ( $\text{HNO}_3(\text{NAT})$  in  $\text{mol mol}^{-1}$ ):

$$\text{HNO}_3(\text{NAT}) = \frac{(e_{\text{HNO}_3(\text{total})} - E_{\text{HNO}_3}^{\text{NAT}})}{p} \quad (2)$$

with  $p$  the ambient pressure (in Pa). It takes place, if *phase* is set to 2 or to 3.

The submodel PSC  
in EMAC

O. Kirner et al.

Title Page

Abstract

Introduction

Conclusions

References

Tables

Figures

◀

▶

◀

▶

Back

Close

Full Screen / Esc

Printer-friendly Version

Interactive Discussion



## 3.2.2 Kinetic growth NAT parameterisation

### Growth and contraction of NAT particles with the aid of a surface growth factor

The kinetic growth NAT parameterisation assumes that the homogeneous NAT formation starts from STS. The phase concept is therefore not required in this approach.

NAT particles initially form with a radius of 0.1  $\mu\text{m}$  and a particle number density of  $1.5 \times 10^{-5}$  particles  $\text{cm}^{-3}$  when the temperature is below  $T_{\text{NAT}}$  (Hanson and Mauersberger, 1988). With the help of the PSC submodel namelists, it is also possible to set necessary supersaturations for the initial NAT formation (see Sect. 4).

After initialisation, the kinetic growth NAT parameterisation uses a surface growth factor ( $G$  in  $\text{m}^2 \text{s}^{-1}$ ) based on Carslaw et al. (2002) to calculate the growth and contraction of NAT. The time-related growth of the NAT particles is a function of this surface growth factor and of the particle radius ( $r$  in m):

$$\frac{dr}{dt} = \frac{G}{r} \quad (3)$$

with

$$G = \frac{D_{\text{HNO}_3}^* M_{\text{NAT}}}{\rho_{\text{NAT}} R_{\text{gas}} T} \left( e_{\text{HNO}_3} - E_{\text{HNO}_3}^{\text{NAT}} \right) \quad (4)$$

This equation describes the dependency of the surface growth factor from the temperature ( $T$  in K), the difference between the partial  $\text{HNO}_3$  vapour pressure ( $e_{\text{HNO}_3}$  in Pa) and the saturation vapour pressure of  $\text{HNO}_3$  over NAT ( $E_{\text{HNO}_3}^{\text{NAT}}$  in Pa), as well as from the diffusion coefficient of  $\text{HNO}_3$  in air ( $D_{\text{HNO}_3}^*$  in  $\text{m}^2 \text{s}^{-1}$ ). The molar mass of NAT ( $M_{\text{NAT}} = 0.117 \text{ kg mol}^{-1}$ ), the universal gas constant ( $R_{\text{gas}} = 8.314 \text{ J mol}^{-1} \text{ K}^{-1}$ ) and the crystal mass density of NAT ( $\rho_{\text{NAT}} = 1626 \text{ kg m}^{-3}$ ) are constants. For positive  $G$ , the radii of the NAT particles increase, through condensation of  $\text{HNO}_3$ . For negative  $G$ , the particles contract through evaporation.

Title Page

Abstract

Introduction

Conclusions

References

Tables

Figures

⏪

⏩

◀

▶

Back

Close

Full Screen / Esc

Printer-friendly Version

Interactive Discussion



$D_{\text{HNO}_3}^*$  is calculated to account for mass transfer non continuum effects for particles with sizes similar to the mean free path (Carslaw et al., 2002):

$$D_{\text{HNO}_3}^* = \frac{D_{\text{HNO}_3}}{1 + 4 D_{\text{HNO}_3} / (v_{\text{HNO}_3} r)} \quad (5)$$

where  $D_{\text{HNO}_3}$  (in  $\text{m}^2 \text{s}^{-1}$ ) is the diffusion coefficient of  $\text{HNO}_3$  in air and  $v_{\text{HNO}_3}$  (in  $\text{m s}^{-1}$ ) is the mean molecular speed.

### Growth of NAT particles over size bins

With the aid of the surface growth factor it is possible to simulate the growth and evaporation of NAT particles. For integration of this growth concept in EMAC, which is an Eulerian model, it is necessary to split the NAT particles into different size bins. In the kinetic growth NAT parameterisation of the submodel PSC consequently a separation into eight size bins is implemented (see Table 1). These are based on a PSC algorithm in the chemistry transport model (CTM) TM5 described by van den Broek et al. (2004).

For every size bin a minimum, a maximum and a mean radius ( $r_{\text{NAT}(\text{bin})}$  in  $\mu\text{m}$ ) exist, as well as a maximum number density (in particles  $\text{cm}^{-3}$ ). The separation of the size bins is based on observations by aircraft, performed in the Arctic winter 1999/2000 by Fahey et al. (2001). They observed a total number density of NAT particles of  $2.3 \times 10^{-4}$  particles  $\text{cm}^{-3}$ , with radii up to greater than  $10 \mu\text{m}$ .

The mean radii of the eight size bins ( $r_{\text{NAT}(\text{bin})}$ ) used in the PSC submodel are  $0.1 \mu\text{m}$ ,  $0.6 \mu\text{m}$ ,  $1.5 \mu\text{m}$ ,  $4.0 \mu\text{m}$ ,  $7.5 \mu\text{m}$ ,  $10.5 \mu\text{m}$ ,  $14.0 \mu\text{m}$  and  $18.0 \mu\text{m}$  (Table 1). The maximum number densities are  $3.28 \times 10^{-5}$  particles  $\text{cm}^{-3}$  in the size bins 1–6 and  $1.64 \times 10^{-5}$  particles  $\text{cm}^{-3}$  in the size bins 7 and 8.

To use this size bin concept additional tracers have been defined in EMAC. The mixing ratio of  $\text{HNO}_3$  containing in NAT ( $\text{HNO}_3(\text{NAT})$ ) had to be split up in eight tracers

Title Page

Abstract

Introduction

Conclusions

References

Tables

Figures

◀

▶

◀

▶

Back

Close

Full Screen / Esc

Printer-friendly Version

Interactive Discussion



( $\text{HNO}_3(\text{NAT})_{(\text{bin})}$  in  $\text{mol mol}^{-1}$ , one tracer per size bin) to ensure transport and diffusion for the NAT particles.

The distribution of the NAT particles to the size bins are calculated in a loop from size bin 1 to size bin 8.

In a first step the initial number density of NAT in the size bin ( $N_{\text{NAT}(\text{bin})\text{ini}}$ ) is calculated from the initial  $\text{HNO}_3(\text{NAT})_{(\text{bin})\text{ini}}$  with the aid of the initial mass of one NAT particle ( $m_{\text{p}(\text{bin})\text{ini}}$  in kg) with the mean radius of this size bin ( $r_{\text{NAT}(\text{bin})}$ ):

$$N_{\text{NAT}(\text{bin})\text{ini}} = \frac{\text{HNO}_3(\text{NAT})_{(\text{bin})\text{ini}} M_{\text{NAT}}}{m_{\text{p}(\text{bin})\text{ini}} N_A} \quad (6)$$

with  $N_A$ , the Avogadro constant ( $6.022 \times 10^{23} \text{ mol}^{-1}$ ) and with

$$m_{\text{p}(\text{bin})\text{ini}} = \frac{4}{3} \pi \rho_{\text{NAT}} r_{\text{NAT}(\text{bin})}^3 \quad (7)$$

If in size bin 1 the mixing ratio of  $\text{HNO}_3(\text{NAT})_{(1)}$  is equal to zero and the temperature is below  $T_{\text{NAT}}$  (Hanson and Mauersberger, 1988), supersaturation can be adjusted via the PSC namelists)  $N_{\text{NAT}(1)\text{ini}}$  will be set to  $1.5 \times 10^{-5} \text{ particles cm}^{-3}$ .

In a second step a new radius ( $r_{\text{new}(\text{bin})}$ ) for the size bin is calculated with the aid of the integrated form of Eq. (3):

$$r_{\text{new}(\text{bin})} = \sqrt{r_{\text{NAT}(\text{bin})}^2 + 2G \Delta t} \quad (8)$$

with the surface growth factor  $G$  (Eq. 4) and  $\Delta t$ , the time step (in s).

With  $r_{\text{new}(\text{bin})}$  it is possible to calculate the new mass of one particle  $m_{\text{p}(\text{bin})\text{new}}$  according to Eq. (7) and the new mixing ratio of  $\text{HNO}_3$  contained in NAT ( $\text{HNO}_3(\text{NAT})_{(\text{bin})\text{new}}$ ):

$$\text{HNO}_3(\text{NAT})_{(\text{bin})\text{new}} = \text{HNO}_3(\text{NAT})_{(\text{bin})\text{ini}} \frac{m_{\text{p}(\text{bin})\text{new}}}{m_{\text{p}(\text{bin})\text{ini}}} \quad (9)$$

Title Page

Abstract

Introduction

Conclusions

References

Tables

Figures

⏪

⏩

◀

▶

Back

Close

Full Screen / Esc

Printer-friendly Version

Interactive Discussion



The new number density for NAT particles of the current size bin ( $N_{\text{NAT}(\text{bin})}$ ) with the corresponding mean radius is calculated with

$$N_{\text{NAT}(\text{bin})} = \frac{\text{HNO}_3(\text{NAT})_{(\text{bin})\text{new}} M_{\text{NAT}}}{r_{\text{NAT}(\text{bin})} N_A} \quad (10)$$

If  $N_{\text{NAT}(\text{bin})}$  is larger than the maximum number density of the current size bin, the overrun will be transferred to the next larger size bin by transformation into the corresponding number density of NAT particles with the mean radius of this larger size bin. The overrun is also considered in the calculation of  $\text{HNO}_3(\text{NAT})_{(\text{bin})\text{new}}$  (Eq. 9).

After the loop over all size bins, it is possible to calculate the total  $\text{HNO}_3(\text{NAT})$  as the sum of all  $\text{HNO}_3(\text{NAT})_{(\text{bin})}$ :

$$\text{HNO}_3(\text{NAT}) = \sum_{\text{bin}=1}^8 \text{HNO}_3(\text{NAT})_{(\text{bin})} \quad (11)$$

### 3.3 The parameterisation of ice particles

For the formation of ice particles (type 2 PSC) there is only one parameterisation in the submodel PSC. It is based on the thermodynamical approach of Marti and Mauersberger (1993).

If *phase* is set to 3, the water fraction in ice particles ( $\text{H}_2\text{O}(\text{ice})$  in  $\text{mol mol}^{-1}$ ) is calculated as difference of the total partial pressure of  $\text{H}_2\text{O}$  ( $e_{\text{H}_2\text{O}(\text{total})}$  in Pa) and the saturation vapour pressure of  $\text{H}_2\text{O}$  over ice particles ( $E_{\text{H}_2\text{O}}^{\text{ice}}$  in Pa), which depends on pressure and temperature:

$$\text{H}_2\text{O}(\text{ice}) = \frac{(e_{\text{H}_2\text{O}(\text{total})} - E_{\text{H}_2\text{O}}^{\text{ice}})}{p} \quad (12)$$

Title Page

Abstract

Introduction

Conclusions

References

Tables

Figures

◀

▶

◀

▶

Back

Close

Full Screen / Esc

Printer-friendly Version

Interactive Discussion



### 3.4 The calculation of surfaces, number densities and mean radii of PSC particles

For the calculation of the reaction coefficients ( $\kappa$ ) of the heterogeneous reactions (see Sect. 3.5), which take place on the surface of the solid PSC particles as well as on the surface of the liquid stratospheric aerosols (STS and SSA), it is necessary to calculate the total surface of liquid aerosols, NAT and ice particles.

#### 3.4.1 Surfaces and mean radii of liquid droplets

In the parameterisation for liquid droplets after Carslaw et al. (1995b) the total surface ( $A_{\text{liq}}$ ) and the mean radius ( $r_{\text{liq}}$ ) are simulated for the calculation of the heterogeneous reaction coefficients.

To calculate  $A_{\text{liq}}$ , first the total mass of the liquid phase per air volume ( $m_{\text{total}}$  in  $\text{g cm}^{-3}$ ) is calculated. After this, the computation of the mass density of the liquid phase ( $\text{dens}_{\text{liq}}$  in  $\text{g cm}^{-3}$ ) is possible. With the equation

$$V_{\text{liq}} = \frac{m_{\text{total}}}{\text{dens}_{\text{liq}}} \quad (13)$$

the total volume of the liquid droplets per air volume ( $V_{\text{liq}}$  in  $\text{cm}^3 \text{cm}^{-3}$ ) is calculated and also the total surface of the liquid stratospheric aerosols per air volume ( $A_{\text{liq}}$  in  $\text{cm}^2 \text{cm}^{-3}$ ) following Grainger et al. (1995):

$$A_{\text{liq}} = 8.406 V_{\text{liq}}^{0.751} \quad (14)$$

The mean radius of the liquid aerosols ( $r_{\text{liq}}$  in cm) is calculated with the relation of the effective radius ( $r_{\text{eff}}$ ), the volume of the aerosol droplets ( $V_{\text{liq}}$ ) and the proportion of  $r_{\text{liq}}$  and  $r_{\text{eff}}$  assuming a logarithmic Gaussian distribution with the following parameterisations after Grainger et al. (1995):

$$r_{\text{liq}} = r_{\text{eff}} e^{-0.173} \quad (15)$$

Title Page

Abstract

Introduction

Conclusions

References

Tables

Figures

◀

▶

◀

▶

Back

Close

Full Screen / Esc

Printer-friendly Version

Interactive Discussion



with  $r_{\text{eff}} = 0.357 V_{\text{liq}}^{0.249}$  (16)

$A_{\text{liq}}$  is used in the calculation of the heterogeneous reaction coefficients ( $\kappa$ ) on stratospheric liquid aerosols in Eq. (21).

### 3.4.2 Total number density and mean radius of solid particles using the thermodynamical NAT parameterisation

Using the thermodynamical NAT parameterisation, the total number density ( $N_{\text{solid}}$  in particles  $\text{m}^{-3}$ ) and the mean radius ( $r_{\text{solid}}$  in m) instead of the total surface of the solid particles are calculated.

With the help of  $\text{H}_2\text{O}(\text{ice})$  (Eq. 12) and  $\text{HNO}_3(\text{NAT})$  (Eq. 2) the total mass of solid particles ( $m_{\text{solid}}$ ) as well as their total volume ( $V_{\text{solid}}$  in  $\text{m}^3$ ) is calculated. The total number density of the solid particles ( $N_{\text{solid}}$ ) is then:

$$N_{\text{solid}} = \max\left(\frac{3 V_{\text{solid}}}{4 \pi r_{\text{min}}^3}, N_{\text{max}}\right) \quad (17)$$

The minimum radius ( $r_{\text{min}}$  in m) is from the PSC submodel namelists (see Sect. 4).  $N_{\text{solid}}$  is compared with a maximum number density ( $N_{\text{max}}$ ), also determined in the PSC submodel namelists. If  $N_{\text{solid}}$  is greater than  $N_{\text{max}}$ , then  $N_{\text{solid}}$  is set to  $N_{\text{max}}$  (if this is the case,  $r_{\text{solid}}$  will be greater than  $r_{\text{min}}$  (see Eq. 18).

With the help of  $N_{\text{solid}}$  the mean radius ( $r_{\text{solid}}$ ) is calculated:

$$r_{\text{solid}} = \sqrt[3]{\frac{3 V_{\text{solid}}}{4 \pi N_{\text{solid}}}} \quad (18)$$

Within the thermodynamical NAT parameterisation  $N_{\text{solid}}$  and  $r_{\text{solid}}$  are used for the calculation of the reaction coefficients ( $\kappa$ ) of heterogeneous reactions on the surface of ice and NAT particles (see Eq. 24).  $N_{\text{solid}}$  is the sum of ice and NAT particles and  $r_{\text{solid}}$  the mean radius of all solid particles.

Title Page

Abstract

Introduction

Conclusions

References

Tables

Figures

◀

▶

◀

▶

Back

Close

Full Screen / Esc

Printer-friendly Version

Interactive Discussion



### 3.4.3 Total number density and mean radius of NAT and ice particles using the kinetic growth NAT parameterisation

In contrast to the thermodynamical NAT approach, in the kinetic growth NAT parameterisation the number densities of NAT ( $N_{\text{NAT}}$ ) and ice particles ( $N_{\text{ice}}$ ), as well as the mean radii of NAT particles ( $r_{\text{NAT}}$ ) and ice particles ( $r_{\text{ice}}$ ) are used for the calculation of the heterogeneous reaction coefficients ( $\kappa$ ) on the surface of NAT (Eq. 25) and ice particles (Eq. 26).

The number density of NAT is calculated from the single number density in each size bin ( $N_{\text{NAT,bin}}$ ):

$$N_{\text{NAT}} = \sum_{\text{bin}=1}^8 N_{\text{NAT}(\text{bin})} \quad (19)$$

The mean NAT radius of all particles is calculated from the radii of each size bin ( $r_{\text{NAT,bin}}$ ), weighted with the NAT number density:

$$r_{\text{NAT}} = \sqrt{\left( \sum_{\text{bin}=1}^8 N_{\text{NAT}(\text{bin})} \cdot r_{\text{NAT}(\text{bin})}^2 \right) / N_{\text{NAT}}} \quad (20)$$

The number density of ice particles ( $N_{\text{ice}}$ ) and their radius ( $r_{\text{ice}}$ ) are defined in the same way as  $N_{\text{solid}}$  (Eq. 17) and  $r_{\text{solid}}$  (Eq. 18).

### 3.5 The calculation of heterogeneous chemistry reaction coefficients

The reaction coefficients for the heterogeneous reactions on PSCs (see Reactions R1–R11) are calculated in the PSC submodel. After calculation the reaction coefficients are delivered to the chemistry submodel MECCA1 (Sander et al., 2005). In MECCA1 the corresponding heterogeneous chemistry is simulated.

Title Page

Abstract

Introduction

Conclusions

References

Tables

Figures

◀

▶

◀

▶

Back

Close

Full Screen / Esc

Printer-friendly Version

Interactive Discussion



### 3.5.1 Liquid droplets

The second order heterogeneous reaction coefficient<sup>1</sup> ( $\kappa$  in  $\text{cm}^3 \text{s}^{-1}$ ) for liquid stratospheric aerosol (STS and SSA) is calculated in a first step as a heterogeneous reaction coefficient of first order<sup>2</sup> ( $\kappa'$  in  $1 \text{ s}^{-1}$ , Hanson et al., 1996):

$$\kappa' = \frac{\gamma \cdot c_{\text{bar}} \cdot A_{\text{liq}}}{4} \quad (21)$$

with  $\gamma$  the reaction probability,  $A_{\text{liq}}$  the surface of the liquid droplets (see Eq. 14) and  $c_{\text{bar}}$  an auxiliary variable (see Eq. 22). Thereby  $\gamma$  depends on the radius of the liquid aerosols and on the mixing ratios of the substances in the gas phase involved in the reaction. For the specific heterogeneous reaction is calculated after Carslaw et al. (1995b), Luo et al. (1995), Hanson and Ravishankara (1994) and Hanson et al. (1996).

The variable  $c_{\text{bar}}$  (in  $\text{m}^{-2} \text{s}^{-1}$ ) depends on a constant ( $c$ ) and on temperature ( $T$ ):

$$c_{\text{bar}} = c \sqrt{T} \quad (22)$$

According to the specific heterogeneous reaction, the constant  $c$  is in the range between 1221.4 (Reaction R6) and 1616.0 (Reaction R11). For more details see Carslaw et al. (1995b).

The heterogeneous reactions (Reactions R1–R11) are bimolecular reactions, with one educt in gas phase and one educt in liquid phase. To get  $\kappa$  (in  $\text{cm}^3 \text{s}^{-1}$ ) from  $\kappa'$  (in  $1 \text{ s}^{-1}$ ) it is necessary to divide  $\kappa'$  through the gases phase concentration of the substance in liquid phase (respectively solid phase by NAT and ice, see below). For example for Reaction (R1):



<sup>1</sup>true for bimolecular reactions

<sup>2</sup>true for monomolecular reactions

Title Page

Abstract

Introduction

Conclusions

References

Tables

Figures

◀

▶

◀

▶

Back

Close

Full Screen / Esc

Printer-friendly Version

Interactive Discussion



$\kappa$  is calculated as:

$$\kappa = \frac{\kappa'}{[\text{H}_2\text{O}]} \quad (23)$$

This calculation is possible, as the concentration of  $\text{H}_2\text{O}$  is much higher as the concentration of  $\text{N}_2\text{O}_5$  and the concentration of  $\text{H}_2\text{O}$  is more or less independent of the reaction. The concentration of  $\text{N}_2\text{O}_5$  is therefore the limiting factor.

### 3.5.2 Solid NAT and ice particles using the thermodynamical NAT parameterisation

Using the thermodynamical PSC parameterisation the first step of the calculation of  $\kappa$  (in  $\text{cm}^3 \text{s}^{-1}$ ) on NAT and ice particles is to calculate  $\kappa'$  (in  $1 \text{s}^{-1}$ ) with  $N_{\text{solid}}$  and  $r_{\text{solid}}$ :

$$\kappa'(r) = \frac{4.56 \times 10^4 \gamma \sqrt{\frac{T}{M_A}} r_{\text{solid}}^2 N_{\text{solid}}}{1 + 3.3 \times 10^4 \gamma r_{\text{solid}} \frac{\rho}{T}} \quad (24)$$

with  $M_A$  the molecular mass of substance A (educt of heterogeneous reaction in gas phase, in  $\text{g mol}^{-1}$ ),  $T$  the temperature (in K),  $\rho$  the pressure (in hPa),  $r_{\text{solid}}$  the radius of solid particles (in cm, see Eq. 18),  $N_{\text{solid}}$  the number density of solid particles (in particles  $\text{cm}^{-3}$ ) (see Eq. 17) and  $\gamma$  the reaction probability (see Table 2). For more details of Eq. (24) see Müller (1994) and Turco et al. (1989).

To get  $\kappa$  for the specific heterogeneous reaction, it is necessary to divide  $\kappa'$  (see Eq. 23) by the gas phase concentration of the substance contained in solid phase as educt in the heterogeneous reaction.

The reaction probabilities ( $\gamma$ ) of the reactions on NAT and ice particles used in the PSC submodel are described in Table 2. Most of the reaction probabilities are from Sander et al. (2003, 2006). The others are transferred from the original code of the PSC submodel which is based on the “Mainz Stratospheric Box Model” (Carslaw et al., 1994).

Title Page

Abstract

Introduction

Conclusions

References

Tables

Figures

◀

▶

◀

▶

Back

Close

Full Screen / Esc

Printer-friendly Version

Interactive Discussion



### 3.5.3 Solid NAT and ice particles using the kinetic growth NAT parameterisation

Using the kinetic growth NAT parameterisation, the heterogeneous reaction coefficients (second order,  $\kappa$ ) for NAT particles are also calculated with Eq. (24). In this case neither  $N_{\text{solid}}$  nor  $r_{\text{solid}}$  are used, but  $N_{\text{NAT}}$  and  $r_{\text{NAT}}$ . The calculation of  $\kappa^l$  on NAT particles is then:

$$k^l(r) = \frac{4.56 \times 10^4 \gamma \sqrt{\frac{T}{M_A}} r_{\text{NAT}}^2 N_{\text{NAT}}}{1 + 3.3 \times 10^4 \gamma r_{\text{NAT}} \frac{\rho}{T}} \quad (25)$$

with  $r_{\text{NAT}}$  the mean radius of NAT particles (in cm),  $N_{\text{NAT}}$  the number density of NAT particles (in particles  $\text{cm}^{-3}$ ) and  $\gamma$  the reaction probability on NAT particles (see Table 2).

The calculation of  $\kappa^l$  on ice particles uses  $N_{\text{ice}}$  and  $r_{\text{ice}}$  instead of  $N_{\text{solid}}$  and  $r_{\text{solid}}$  in Eq. (24):

$$k^l(r) = \frac{4.56 \times 10^4 \gamma \sqrt{\frac{T}{M_A}} r_{\text{ice}}^2 N_{\text{ice}}}{1 + 3.3 \times 10^4 \gamma r_{\text{ice}} \frac{\rho}{T}} \quad (26)$$

with  $r_{\text{ice}}$  the mean radius of ice particles (in cm),  $N_{\text{ice}}$  the number density of ice particles (in particles  $\text{cm}^{-3}$ ) and  $\gamma$  the reaction probability on ice particles (see Table 2).

In order to get  $\kappa$  for the specific heterogeneous reaction, it is necessary to divide  $\kappa^l$  (see Eq. 23) through the gas phase concentration of the substance presented in solid phase as educt in the heterogeneous reaction.

### 3.6 The sedimentation of PSC-particles

Depending on the applied PSC parameterisation the calculation of sedimentation is performed for solid particles (thermodynamical NAT parameterisation) or for NAT and

Title Page

Abstract

Introduction

Conclusions

References

Tables

Figures

◀

▶

◀

▶

Back

Close

Full Screen / Esc

Printer-friendly Version

Interactive Discussion



ice particles (kinetic growth NAT parameterisation). In each case the sedimentation can be separated into different parts.

After the calculation of the sedimentation velocity of the PSC particles, the range of the sedimentation path during one time step is calculated. Thereafter the change of mass fraction of the PSC particles per time step and grid box, as well as the changes of H<sub>2</sub>O and HNO<sub>3</sub> in the gas phase are determined.

### 3.6.1 Calculation of the sedimentation velocity

#### Sedimentation velocity using the thermodynamical NAT parameterisation

Using the thermodynamical NAT parameterisation the sedimentation velocity is calculated for solid particles ( $v_{\text{sed(solid)}}$  in  $\text{m s}^{-1}$ ) with the parameterisation of Waibel (1997). In this parameterisation in a first step the calculation of an auxiliary velocity ( $v_y$  in  $\text{m s}^{-1}$ ) takes place:

$$v_y = \frac{g \rho_{\text{ice}} r_{\text{solid}}^2}{4.5 \cdot \eta T} \quad (27)$$

with  $g$  the acceleration of gravity ( $9.80665 \text{ m s}^{-2}$ ),  $\rho_{\text{ice}}$  the density of ice particles ( $990.0 \text{ kg m}^{-3}$ ),  $r_{\text{solid}}$  the mean radius of solid particles (in m),  $T$  the temperature (in K) and a factor  $\eta$  ( $6.45 \times 10^{-8} \text{ kg m}^{-1} \text{ s}^{-1} \text{ K}^{-1}$ ). The sedimentation velocity for solid particles is calculated in a second step from  $v_y$  (in  $\text{m s}^{-1}$ ) and the variable  $\text{val}_x$  (dimensionless):

$$v_{\text{sed(solid)}} = 0.893 v_y \text{val}_x \quad (28)$$

with

$$\text{val}_x = 1 + \frac{\alpha_1 T}{\rho r_{\text{solid}}} + \frac{\alpha_2 T e^{-\frac{p}{\alpha_3 T} r_{\text{solid}}}}{\rho r_{\text{solid}}} \quad (29)$$

Title Page

Abstract

Introduction

Conclusions

References

Tables

Figures

◀

▶

◀

▶

Back

Close

Full Screen / Esc

Printer-friendly Version

Interactive Discussion



and  $p$  the pressure (in Pa) as well as the auxiliary variables  $\alpha_1 = 1.49 \times 10^{-5} \text{ m Pa K}^{-1}$ ,  $\alpha_2 = 5.02 \times 10^{-6} \text{ m Pa K}^{-1}$  and  $\alpha_3 = 2.64 \times 10^{-5} \text{ m Pa K}^{-1}$ .

## Sedimentation velocity using the kinetic growth NAT parameterisation

Using the kinetic growth PSC parameterisation, the sedimentation velocity is not calculated for solid particles but for NAT and ice particles. The calculation of the sedimentation velocity for ice particles ( $v_{sed(ice)}$  in  $\text{m s}^{-1}$ ) is performed with  $r_{ice}$  using the parameterisation of Waibel (1997) described in the Eqs. (27)–(29).

The sedimentation velocity for NAT particles ( $v_{sed(NAT)}$  in  $\text{m s}^{-1}$ ) is based on Carslaw et al. (2002). The sedimentation velocity is calculated for every NAT size bin ( $v_{sed(NAT)(bin)}$ ).  $v_{sed(NAT)(bin)}$  depends on the mean radius of the NAT size bin ( $r_{NAT(bin)}$ ) and on a sedimentation factor ( $S$  in  $1 \text{ ms}^{-1}$ ):

$$v_{sed(NAT)(bin)} = S r_{NAT(bin)}^2 \quad (30)$$

with

$$S = \frac{2g\rho_{NAT}C_c}{9\eta_a} \quad (31)$$

with  $g$  the acceleration of gravity ( $9.80665 \text{ m s}^{-2}$ ),  $\rho_{NAT}$  the crystal mass density of NAT ( $1626 \text{ kg m}^{-3}$ ),  $C_c$  the ‘‘Cunningham slip flow correction factor’’ (dimensionless) and  $\eta_a$  the viscosity of air (in  $\text{g ms}^{-1}$ ).

The correction factor  $C_c$  is calculated by:

$$C_c = 1 + \frac{l_{HNO_3}}{r_{NAT(bin)}} \left[ 1.257 + 0.4e^{\left(\frac{-1.1r_{NAT(bin)}}{l_{HNO_3}}\right)} \right] \quad (32)$$

with  $l_{HNO_3}$  the mean free path of the  $HNO_3$ -particles (in m) (Carslaw et al., 2002).

Title Page

Abstract

Introduction

Conclusions

References

Tables

Figures

◀

▶

◀

▶

Back

Close

Full Screen / Esc

Printer-friendly Version

Interactive Discussion



### 3.6.2 Calculation of the range of the sedimentation path (sedimentation step)

The vertical distance of a falling particle per time step is calculated by using the sedimentation velocity. As the vertical coordinate is pressure, this sedimentation step is a pressure difference (SedStep in Pa).

$$\text{SedStep} = \frac{gM_{\text{air}}\rho V_{\text{sed}}\Delta t}{R_{\text{gas}}T} \quad (33)$$

with  $M_{\text{air}}$  the molar mass of air ( $0.02897 \text{ kg mol}^{-1}$ ),  $\rho$  the pressure (in Pa),  $R_{\text{gas}}$  the universal gas constant ( $8.31 \text{ J K mol}^{-1}$ ),  $T$  the temperature (in K) and  $\Delta t$  the time step (in s).

SedStep is calculated for solid particles ( $\text{SedStep}_{\text{solid}}$ ) by using the thermodynamical NAT parameterisation and for ice particles ( $\text{SedStep}_{\text{ice}}$ ) as well as for NAT particles with respect to every size bin ( $\text{SedStep}_{\text{NAT}(\text{bin})}$ ) when using the kinetic growth NAT parameterisation.

### 3.6.3 Calculation of the changes in gas phase $\text{H}_2\text{O}$ and $\text{HNO}_3$ due to sedimentation

With the help of SedStep the changes of the mixing ratios of  $\text{H}_2\text{O}$  and  $\text{HNO}_3$  in gas phase due to ice or NAT sedimentation are calculated. There are three different sedimentation schemes in EMAC available: the “Simple Upwind Scheme”, the “Walcek2000 Scheme” (Walcek, 2000) and the “Trapezoid Scheme” (Buchholz, 2005). In the PSC submodel namelists (see Sect. 4) it is possible to choose one of it.

For example, using the “Simple Upwind Scheme” and the kinetic growth parameterisation the change of  $\text{HNO}_3$  is calculated for every size bin ( $\text{HNO}_{3(\text{chg}(\text{bin},k))}$ ):

$$\text{HNO}_{3(\text{chg}(\text{bin},k))} = \frac{\text{HNO}_{3(\text{bin},k-1)} \text{SedStep}_{\text{NAT}(\text{bin},k-1)}}{\rho_{\text{bot}(k)} - \rho_{\text{top}(k)}} - \frac{\text{HNO}_{3(\text{bin},k)} \text{SedStep}_{\text{NAT}(\text{bin},k)}}{\rho_{\text{bot}(k)} - \rho_{\text{top}(k)}} \quad (34)$$

Title Page

Abstract

Introduction

Conclusions

References

Tables

Figures

◀

▶

◀

▶

Back

Close

Full Screen / Esc

Printer-friendly Version

Interactive Discussion



$p_{\text{bot}(k)}$  and  $p_{\text{top}(k)}$  are the pressures at the top and the bottom of the relevant grid box  $k$  ( $k - 1$  means the grid box above grid box  $k$ ),  $\text{SedStep}_{\text{NAT}(\text{bin},k)}$  the sedimentation step of NAT and  $\text{HNO}_3(\text{bin},k)$  the  $\text{HNO}_3$  mixing ratio of the current size bin in this grid box. The total change in  $\text{HNO}_3$  is the sum over all size bins:

$$5 \quad \text{HNO}_3(\text{chg}(k)) = \sum_{\text{bin}=1}^8 \text{HNO}_3(\text{chg}(\text{bin},k)) \quad (35)$$

The new  $\text{HNO}_3$  mixing ratio is calculated as:

$$\text{HNO}_3(\text{new}(k)) = \text{HNO}_3(\text{old}(k)) + \text{HNO}_3(\text{chg}(k)) \quad (36)$$

For the changes in  $\text{H}_2\text{O}$  ( $\text{H}_2\text{O}_{(\text{chg}(k))}$ ) the same calculations are performed, but with the sedimentation step of ice particles ( $\text{SedStep}_{\text{ice}}$ ).

10 Using the thermodynamical NAT parameterisation the changes of  $\text{H}_2\text{O}$  and  $\text{HNO}_3$  are calculated with the sedimentation step of solid particles ( $\text{SedStep}_{\text{solid}}$ ).

The “Walcek2000 Scheme” and the “Trapezoid Scheme”, as well as an assessment of the three sedimentation schemes are described in Buchholz (2005). Buchholz (2005) recommends the “Trapezoid Scheme” applied in the thermodynamical NAT parameterisation. But applying the kinetic growth NAT parameterisation Kirner (2008) recommends the “Simple Upwind Scheme”.

#### 4 Namelists of the submodel PSC

The two namelists of the PSC submodel are presented in Table 3. The CTRL namelist contains parameters for the internal control of the PSC submodel, the CPL namelist variables are important for coupling with other submodels. With these namelists it is possible to setup the submodel PSC with different parameters.

The most essential parameter in the PSC CTRL namelist is *KinPar*. It stands for the option using the described kinetic growth NAT parameterisation ( $\text{KinPar} = T$ ) or the

## The submodel PSC in EMAC

O. Kirner et al.

Title Page

Abstract

Introduction

Conclusions

References

Tables

Figures

◀

▶

◀

▶

Back

Close

Full Screen / Esc

Printer-friendly Version

Interactive Discussion



thermodynamical NAT parameterisation ( $KinPar = F$ ). With the choice of  $KinPar$  some of the other parameters have different meanings.

If  $LAdvectIceNat$  is set to  $T$  advected ice particles have influence on the formation of ice, i.e., if ice particles exist in a grid box,  $phase$  is set to 3 (see Sect. 3.2.1) and no supercooling (see below) is required to form ice particles. The same is valid for the NAT formation, i.e. if NAT particles already exist in a grid box,  $phase$  is set to 2 and no supercooling is required to form NAT. As the phase concept is not valid for NAT formation in the kinetic growth NAT parameterisation ( $KinPar = T$ ),  $LAdvectIceNat$  has in this case no influence.

The parameter  $LHomNucNAT$  has also no influence on the formation of NAT, if  $KinPar$  is set to  $T$ , as in the kinetic growth NAT parameterisation the homogeneous NAT formation is assumed. But if  $KinPar$  is set to  $F$  and  $LHomNucNAT$  is set to  $T$ , homogeneous NAT formation is included in the thermodynamical PSC parameterisation.

For the homogenous NAT formation it is possible to set with  $NatFormThreshold$  a required supercooling (in K). This supercooling has an influence only, if  $LHomNucNAT$  is set to  $T$ , or if the kinetic growth NAT parameterisation is used. In any case  $NatFormThreshold$  is only needed for the first formation of NAT in a grid cell.

With  $minKhet$  and  $maxKhet$  it is possible to set minima and maxima for the heterogeneous reaction coefficients. For example, if the calculated coefficient is greater than  $maxKhet$  the heterogeneous reaction coefficient is limited by  $maxKhet$ . The values of  $minKhet$  and  $maxKhet$  are only relevant, if  $LCalcChem$  (see below) is set to  $T$ .

The parameter  $SupSatIce$  is responsible for the supersaturation for ice formation. It is denoted as a factor, for example a  $SupSatIce$  value of 1.5 means that the  $H_2O$  partial pressure must be 50% higher as the  $H_2O$  saturation pressure to form ice particles. The supersaturation should be reduced for coarse resolutions.

The parameters minimum radius ( $r_{min}$ ) and maximum number density ( $N_{max}$ ) are relevant for the calculation of the mean radius and number density of PSC particles. They are essential for the number density of solid particles using the thermodynamical NAT parameterisation or for ice particles using the kinetic growth NAT parameterisation,

## The submodel PSC in EMAC

O. Kirner et al.

Title Page

Abstract

Introduction

Conclusions

References

Tables

Figures

◀

▶

◀

▶

Back

Close

Full Screen / Esc

Printer-friendly Version

Interactive Discussion



respectively (Eq. 17). The higher  $N_{\max}$  is chosen, the lower is the mean radius and the sedimentation velocity of solid or ice particles, respectively.

With the parameter *SedScheme* the sedimentation scheme for the denitrification and dehydration is chosen. The simple upwind scheme is described in Sect. 3.6.3.

If the parameter *LCalcChem* in the PSC CPL namelist (Table 3) is set to *T*, the heterogeneous reaction coefficients are calculated in the submodel PSC. To transfer this reaction coefficients to the chemistry submodel MECCA1, it is required to set *het\_stream* = “psc” in the CPL namelist of submodel MECCA1.

With the parameter *TempShift* it is possible to change the temperature in the submodel PSC. For example, if *TempShift* is set to -2.0, the polar stratospheric clouds are calculated with temperatures 2.0 K lower as the model temperatures. This can be useful for sensitivity studies.

The parameters  $r_{\text{lat}}$ ,  $r_{\text{lb}}$ ,  $r_{\text{mb}}$  and  $r_{\text{ub}}$  describe the boundaries of the PSC region. Only within this region the calculations concerning the polar stratospheric clouds take place. Thereby  $r_{\text{lat}}$  (in degrees north) describes the borders of the PSC region in the Southern and Northern Hemisphere.  $r_{\text{lb}}$  and  $r_{\text{ub}}$  (in Pa) are the lower and upper boundaries of the Antarctic and Arctic PSC region.  $r_{\text{mb}}$  (in Pa) describes the boundary below which the PSC region is calculated with the help of  $T_{\text{ice}}$  and  $T_{\text{NAT}}$ . Between  $r_{\text{lb}}$  and  $r_{\text{mb}}$  the PSC region is defined, if the condition  $T_{\text{ice}} \leq T_{\text{NAT}}$  is fulfilled.

With the help of the parameter  $I_{\text{feedback}}$  it is possible to switch-off the dynamical-chemical feedback. In this case the total  $\text{HNO}_3$  vapour pressure ( $e_{\text{HNO}_3(\text{total})}$  in Pa) is described through a pre-defined climatology. This  $\text{HNO}_3$  climatology has to be imported, e.g. via the submodel OFFLEM (Kerkweg et al., 2006b).

## 5 Results

In Fig. 1 some results of an EMAC simulation (version 1.7, updated with the new version of submodel psc) using the kinetic growth NAT parameterisation and the parameters of the PSC namelists in Table 3 are shown. During the Antarctic winter 2007 the formation

### The submodel PSC in EMAC

O. Kirner et al.

Title Page

Abstract

Introduction

Conclusions

References

Tables

Figures

◀

▶

◀

▶

Back

Close

Full Screen / Esc

Printer-friendly Version

Interactive Discussion



of type 1a PSC polewards of 87.9° S begins mid May at altitudes between 20 hPa and 40 hPa. After that the NAT particles exist in the maximum range from 180 hPa to 13 hPa and yield number densities of maximal 230 particles m<sup>-3</sup>. Through the sedimentation of NAT particles the denitrification takes place. Thus the mixing ratios of HNO<sub>3</sub> decrease rapidly from May to July at altitudes of the existing type 1a PSC and obtain minima less than 0.5 nmol mol<sup>-1</sup>.

The formation of type 2 PSC starts at the beginning of June and therefore later as type 1a PSC. In the following time the ice particles exist in the maximum range from 180 hPa to 18 hPa and reach number densities of maximal 42 000 particles m<sup>-3</sup>. Through the sedimentation of ice particles the dehydration takes place in the stratosphere. The mixing ratios of H<sub>2</sub>O rapidly decrease from June to August at altitudes with existing ice particles and obtain minima less than 1.0 μmol mol<sup>-1</sup>.

More results including a detailed evaluation of the effects of the thermodynamical and kinetic growth NAT parameterisation on the simulated chemistry will be published by Kirner et al. (2010) elsewhere.

## 6 Conclusions

With the submodel PSC it is possible to simulate the polar stratospheric clouds and their feedbacks to the chemistry including denitrification and dehydration. Due to two different NAT parameterisations and due to various parameters in the PSC namelists the submodel is highly flexible and can be setup according to different scientific theories of PSC formation and development.

*Acknowledgements.* The authors would like to thank Volker Grewe of DLR for his helpful comments on the manuscript.

### The submodel PSC in EMAC

O. Kirner et al.

Title Page

Abstract

Introduction

Conclusions

References

Tables

Figures

◀

▶

◀

▶

Back

Close

Full Screen / Esc

Printer-friendly Version

Interactive Discussion



## References

- Abbatt, J. P. D. and Molina, M.J.: The heterogeneous reaction of HOCl + HCl  $\rightarrow$  Cl<sub>2</sub> + H<sub>2</sub>O on ice and nitric-acid trihydrate – reaction probabilities and stratospheric implications, *Geophys. Res. Lett.*, 19, 461–464, 1992. 2075
- 5 Bertram, A. K., Patterson, D. D., and Sloan, J. J.: Mechanisms and temperatures for the freezing of sulfuric acid aerosols measured by FTIR extinction spectroscopy, *J. Phys. Chem.*, 100, 2376–2383, 1996. 2074
- Beyer, K. D., Seago, S. W., Chang, H. Y., and Molina, M. J.: Composition and freezing of aqueous H<sub>2</sub>SO<sub>4</sub>-HNO<sub>3</sub> solutions under polar stratospheric conditions, *Geophys. Res. Lett.*, 21, 871–874, 1994. 2073
- 10 Biermann, U. M., Crowley, J. N., Huthwelker, T., Moortgat, G. K., Crutzen, P. J., and Peter, T.: FTIR studies on lifetime prolongation of stratospheric ice particles due to NAT coating, *Geophys. Res. Lett.*, 25, 3939–3942, 1998. 2073, 2074
- Buchholz, J.: Simulations of physics and chemistry of polar stratospheric clouds with a general circulation model, Ph.D. thesis, Johannes Gutenberg University Mainz, Germany, 2005. 2078, 2080, 2094, 2095
- 15 Carslaw, K. S., Luo, B. P., Clegg, S. L., Peter, T., Brimblecombe, P., and Crutzen, P. J.: Stratospheric aerosol growth and HNO<sub>3</sub> gas phase depletion from coupled HNO<sub>3</sub> and water uptake by liquid particles, *Geophys. Res. Lett.*, 21, 2479–2482, 1994. 2073, 2090, 2106
- 20 Carslaw, K. S., Clegg, S. L., and Brimblecombe, P.: A thermodynamic model of the system HCl-HNO<sub>3</sub>-H<sub>2</sub>SO<sub>4</sub>-H<sub>2</sub>O including solubilities of HBr, from <200 K to 328 K, *J. Phys. Chem.*, 99, 11557–11574, 1995a. 2073
- Carslaw, K. S., Luo, B., and Peter, T.: An analytic expression for the composition of aqueous HNO<sub>3</sub>-H<sub>2</sub>SO<sub>4</sub> stratospheric aerosols including gas phase removal of HNO<sub>3</sub>, *Geophys. Res. Lett.*, 22(14), 1877–1880, 1995b. 2072, 2078, 2079, 2086, 2089
- 25 Carslaw, K. S., Peter, T., and Clegg, S. L.: Modeling the composition of liquid stratospheric aerosols, *Rev. Geophys.*, 35, 125–154, 1997. 2073, 2079
- Carslaw, K. S. Wirth, M., Tsias, A., Luo, B. P., Dörnbrack, A., Leutbecher, M., Volkert, H., Renger, W., Bacmeister, J. T., and Peter, T.: Particle microphysics and chemistry in remotely observed mountain polar stratospheric clouds, *J. Geophys. Res.*, 103(D5), 5785–5796, doi:10.1029/97JD03626, 1998. 2073, 2074, 2075, 2081
- 30 Carslaw, K. S., Kettleborough, J. A., Northway, M. J., Davies, S., Gao, R. S., Fahey, D. W.,

**GMDD**

3, 2071–2108, 2010

## The submodel PSC in EMAC

O. Kirner et al.

[Title Page](#)

[Abstract](#)

[Introduction](#)

[Conclusions](#)

[References](#)

[Tables](#)

[Figures](#)

[◀](#)

[▶](#)

[◀](#)

[▶](#)

[Back](#)

[Close](#)

[Full Screen / Esc](#)

[Printer-friendly Version](#)

[Interactive Discussion](#)



- Baumgardner, D. G., Chipperfield, M. P., and Kleinböhl, A.: A vortex-scale simulation of the growth and sedimentation of large nitric acid hydrate particles, *J. Geophys. Res.*, 107(D20), 8300, doi:10.1029/2001JD000467, 2002. 2072, 2073, 2074, 2078, 2080, 2082, 2083, 2093
- Crutzen, P. J., Müller, R., Brühl, C., and Peter, T.: On the potential importance of the gas-phase reaction  $\text{CH}_3\text{O}_2 + \text{ClO} \rightarrow \text{ClOO} + \text{CH}_3\text{O}$  and the heterogeneous reaction  $\text{HOCl} + \text{HCl} \rightarrow \text{H}_2\text{O} + \text{Cl}_2$  in ozone hole chemistry, *Geophys. Res. Lett.*, 19, 1113–1116, 1992. 2075, 2078
- Daerden, F., Larsen, N., Chabrillat, S., Errera, Q., Bonjean, S., Fonteyn, D., Hoppel, K., and Fromm, M.: A 3D-CTM with detailed online PSC-microphysics: analysis of the Antarctic winter 2003 by comparison with satellite observations, *Atmos. Chem. Phys.*, 7, 1755–1772, doi:10.5194/acp-7-1755-2007, 2007. 2073, 2074, 2075
- DeMott, P., Rogers, D., and Kreidenweis, S.: The susceptibility of ice formation in upper tropospheric clouds to insoluble aerosol components, *J. Geophys. Res.*, 102, 19575–19584, 1997. 2074, 2075
- Dye, J. E., Baumgardner, D., Gandrud, B. W., Kawa, S. A., Kelly, K. K., Lowenstein, M., Ferry, G. V., Chan, K. R., and Gary, B. L.: Particle size distributions in Arctic polar stratospheric clouds, growth and freezing of sulphuric acid droplets, and implications for cloud formation, *J. Geophys. Res.*, 97, 8015–8034, 1992. 2074
- Fahey, D. W., Gao, R. S., Carslaw, K. S., Kettleborough, J., Popp, P. J., Northway, M. J., Holecek, J. C., Ciciora, S. C., McLaughlin, R. J., Thompson, T. L., Winkler, R. H., Baumgardner, D. G., Gandrud, B., Wennberg, P. O., Dhaniyala, S., McKinney, K., Peter, T., Salawitch, R. J., Bui, T. P., Elkins, J. W., Webster, C. R., Atlas, E. L., Jost, H., Wilson, J. C., Herman, R. L., Kleinböhl, A., and von König, M.: The Detection of Large  $\text{HNO}_3$ -Containing Particles in the Winter Arctic Stratosphere, *Science*, 291, 1026–1031, 2001. 2083
- Fortin, T. J., Drdla, K., Iraci, L. T., and Tolbert, M. A.: Ice condensation on sulfuric acid tetrahydrate: Implications for polar stratospheric ice clouds, *Atmos. Chem. Phys.*, 3, 987–997, doi:10.5194/acp-3-987-2003, 2003. 2074, 2075
- Graedel, T. E. and Crutzen, P. J.: *Atmospheric Change: An Earth System Perspective*, Freeman, New York, 1993. 2077
- Grainger R. G., Lambert, A., Rodgers, C. D., Taylor, F. W., and Desher, T.: Stratospheric aerosol effective radius, surface area and volume estimated from infrared measurements, *J. Geophys. Res.*, 100, 16507–16518, 1995. 2086
- Grooß, J.-U.: Modelling of Stratospheric Chemistry based on HALOE/UARS Satellite Data,

**GMDD**

3, 2071–2108, 2010

## The submodel PSC in EMAC

O. Kirner et al.

[Title Page](#)

[Abstract](#)

[Introduction](#)

[Conclusions](#)

[References](#)

[Tables](#)

[Figures](#)

[⏪](#)

[⏩](#)

[◀](#)

[▶](#)

[Back](#)

[Close](#)

[Full Screen / Esc](#)

[Printer-friendly Version](#)

[Interactive Discussion](#)



**The submodel PSC  
in EMAC**

O. Kirner et al.

[Title Page](#)[Abstract](#)[Introduction](#)[Conclusions](#)[References](#)[Tables](#)[Figures](#)[◀](#)[▶](#)[◀](#)[▶](#)[Back](#)[Close](#)[Full Screen / Esc](#)[Printer-friendly Version](#)[Interactive Discussion](#)

- Ph.D. thesis, Universität Mainz, Germany, 1996. 2078
- Hanson, D. R. and Mauersberger K.: Laboratory studies of the nitric acid trihydrate: implications for the south polar stratosphere, *Geophys. Res. Lett.*, 15, 855–858, 1988. 2072, 2074, 2080, 2081, 2082, 2084
- 5 Hanson, D. R. and Ravishankara, A. R.: The reaction probabilities of  $\text{ClONO}_2$  and  $\text{N}_2\text{O}_5$  on polar stratospheric cloud materials, *J. Geophys. Res.*, 96, 5081–5090, 1991. 2075
- Hanson, D. R. and Ravishankara, A. R.: The reaction of  $\text{ClONO}_2$  with HCl on NAT, NAD, and frozen sulfuric acid and hydrolysis of  $\text{N}_2\text{O}_5$  and  $\text{ClONO}_2$  on frozen sulfuric acid, *J. Geophys. Res.*, 96, 22931–22936, 1993. 2075
- 10 Hanson, D. R. and Ravishankara, A. R.: Reactive uptake of  $\text{ClONO}_2$  onto sulfuric acid due to reaction with HCl and  $\text{H}_2\text{O}$ , *J. Phys. Chem.*, 98, 5728–5735, 1994. 2089
- Hanson, D. R. and Ravishankara, A. R.: Heterogeneous chemistry of Bromine species in sulfuric acid under stratospheric conditions, *Geophys. Res. Lett.*, 22, 385–388, 1995. 2079
- Hanson, D. R., Raishankara, A. R., and Lovejoy, E. R.: Reaction of  $\text{BrONO}_2$  with  $\text{H}_2\text{O}$  on a submicron sulfuric acid aerosol and the implications for the lower stratosphere, *J. Geophys. Res.*, 101, 9063–9069, 1996. 2089
- 15 Huthwelker T., Peter, T., Luo, B. P., Clegg, S. L., Carslaw, K. S., and Brimblecombe, P.: Solubility of HOCl in Water and aqueous  $\text{H}_2\text{SO}_4$  to stratospheric temperatures, *J. Atmos. Chem.*, 21, 81–95, 1995. 2079
- 20 Jensen, E. J. and Toon, O. B.: The potential impact of soot particles from aircraft exhaust on cirrus clouds, *Geophys. Res. Lett.*, 24, 249–252, 1997. 2074, 2075
- Jöckel, P., Sander, R., Kerkweg, A., Tost, H., and Lelieveld, J.: Technical Note: The Modular Earth Submodel System (MESSy) – a new approach towards Earth System Modeling, *Atmos. Chem. Phys.*, 5, 433–444, doi:10.5194/acp-5-433-2005, 2005. 2077
- 25 Jöckel, P., Tost, H., Pozzer, A., Brühl, C., Buchholz, J., Ganzeveld, L., Hoor, P., Kerkweg, A., Lawrence, M. G., Sander, R., Steil, B., Stiller, G., Tanarhte, M., Taraborrelli, D., van Aardenne, J., and Lelieveld, J.: The atmospheric chemistry general circulation model ECHAM5/MESSy1: consistent simulation of ozone from the surface to the mesosphere, *Atmos. Chem. Phys.*, 6, 5067–5104, doi:10.5194/acp-6-5067-2006, 2006. 2077, 2078
- 30 Jöckel, P., Kerkweg, A., Buchholz-Dietsch, J., Tost, H., Sander, R., and Pozzer, A.: Technical Note: Coupling of chemical processes with the Modular Earth Submodel System (MESSy) submodel TRACER, *Atmos. Chem. Phys.*, 8, 1677–1687, doi:10.5194/acp-8-1677-2008, 2008. 2078

- Junge, C. E., Chagnon, C. W., and Manson, J. E.: Stratospheric aerosols, *J. Meteorol.*, 18, 81–108, 1961. 2073
- Kerkweg, A., Buchholz, J., Ganzeveld, L., Pozzer, A., Tost, H., and Jöckel, P.: Technical Note: An implementation of the dry removal processes DRY DEPosition and SEDimentation in the Modular Earth Submodel System (MESSy), *Atmos. Chem. Phys.*, 6, 4617–4632, doi:10.5194/acp-6-4617-2006, 2006a. 2077, 2078
- Kerkweg, A., Sander, R., Tost, H., and Jöckel, P.: Technical note: Implementation of prescribed (OFFLEM), calculated (ONLEM), and pseudo-emissions (TNUDGE) of chemical species in the Modular Earth Submodel System (MESSy), *Atmos. Chem. Phys.*, 6, 3603–3609, doi:10.5194/acp-6-3603-2006, 2006b. 2077, 2097
- Kirner, O.: Prozessstudien der stratosphärischen Chemie und Dynamik mit Hilfe des Chemie-Klima-Modells ECHAM5/MESSy1, Ph.D. thesis, Universität Karlsruhe, Germany, 2008. 2072, 2078, 2080, 2095
- Kirner, O., Ruhnke, R., Höpfner, M., Jöckel, P., and Fischer, H.: A new parameterisation of polar stratospheric clouds (PSC) based on the efficient growth and sedimentation of NAT particles in the chemistry-climate-model EMAC, *Atmos. Chem. Phys.*, in preparation, 2010. 2098
- Koop, T., Luo, B., Tsias, A., and Peter, T.: Water activity as the determinant for homogeneous ice nucleation in aqueous solutions, *Nature*, 406, 611–614, 2000. 2074
- Landgraf, J. and Crutzen, P. J.: An efficient method for online calculations of photolysis and heating rates, *J. Atmos. Sci.*, 55, 863–878, 1998. 2078
- Lowe, D. and MacKenzie, A. R.: Polar stratospheric cloud microphysics and chemistry, *J. Atmos. Sol.-Terr. Phy.*, 70, 13–40, 2008. 2073
- Luo, B. P., Carslaw, K. S., Peter, T., and Clegg, S. L.: Vapor pressures of  $\text{H}_2\text{SO}_4/\text{HNO}_3/\text{HCl}/\text{HBr}/\text{H}_2\text{O}$  solutions to low stratospheric temperatures, *Geophys. Res. Lett.*, 22, 247–250, 1995. 2073, 2079, 2089
- Marti, J. and Mauersberger, K.: A survey and new measurements of ice vapor pressure at temperatures between 170 and 250 K, *Geophys. Res. Lett.*, 20, 363–366, 1993. 2072, 2081, 2085
- Meilinger, S. K.: Heterogeneous Chemistry in the Tropopause Region: Impact of Aircraft Emissions, Ph.D. thesis, Swiss Federal Institute of Technology (ETH), Zürich, Switzerland, 2000. 2078
- Middlebrook, A. M., Tolbert, M. A., and Drdla, K.: Evaporation studies of model polar stratospheric cloud films, *Geophys. Res. Lett.*, 23, 2145–2148, 1996. 2073, 2074

**The submodel PSC  
in EMAC**

O. Kirner et al.

[Title Page](#)[Abstract](#)[Introduction](#)[Conclusions](#)[References](#)[Tables](#)[Figures](#)[◀](#)[▶](#)[◀](#)[▶](#)[Back](#)[Close](#)[Full Screen / Esc](#)[Printer-friendly Version](#)[Interactive Discussion](#)

---

**The submodel PSC  
in EMAC**O. Kirner et al.

---

[Title Page](#)[Abstract](#)[Introduction](#)[Conclusions](#)[References](#)[Tables](#)[Figures](#)[◀](#)[▶](#)[◀](#)[▶](#)[Back](#)[Close](#)[Full Screen / Esc](#)[Printer-friendly Version](#)[Interactive Discussion](#)

- Molina, L. T. and Molina, M. J.: Production of  $\text{Cl}_2\text{O}_2$  from the self-reaction of the ClO-Radical, *J. Phys. Chem.*, 91, 433–436, 1987. 2076
- Müller, R.: Die Chemie des Ozons in der polaren Stratosphäre, Ph.D. thesis, Freie Universität Berlin, Germany, 1994. 2078, 2090
- 5 Roeckner, E., Brokopf, R., Esch, M., Giorgetta, M., Hagemann, S., Koernblueh, L., Manzini, E., Schlese, U., and Schulzweida, U.: Sensitivity of simulated climate to horizontal and vertical resolution in the ECHAM5 atmosphere model, *J. Climate*, 19, 3771–3791, 2006. 2077
- Sander, R., Kerkweg, A., Jöckel, P., and Lelieveld, J.: Technical note: The new comprehensive atmospheric chemistry module MECCA, *Atmos. Chem. Phys.*, 5, 445–450, doi:10.5194/acp-5-445-2005, 2005. 2077, 2088
- 10 Sander, S. P., Friedl, R. R., Ravishankara, A. R., Golden, D. M., Kolb, C. E., Kurylo, M. J., Huie, R. E., Orkin, V. L., Molina, M. J., Moortgat, G. K., and Finlayson-Pitts, B. J.: Chemical Kinetics and Photochemical Data for Use in Atmospheric Studies – Evaluation Number 14, JPL Publication 02-25, Jet Propulsion Laboratory, Pasadena, USA, 2003. 2090, 2106
- 15 Sander, S. P., Finlayson-Pitts, B. J., Friedl, R. R., Golden, D. M., Huie, R. E., Keller-Rudek, H., Kolb, C. E., Kurylo, M. J., Molina, M. J., Moortgat, G. K., Orkin, V. L., Ravishankara, A. R., and Wine, P. W.: Chemical Kinetics and Photochemical Data for Use in Atmospheric Studies – Evaluation Number 15, JPL Publication 06-2, Jet Propulsion Laboratory, Pasadena, 2006. 2090, 2106
- 20 Schlager, H. and Arnold, F.: Measurement of stratospheric gaseous nitric acid in the Winter arctic vortex using a novel rocket-borne mass spectrometer method, *Geophys. Res. Lett.*, 17, 433–436, 1990. 2074
- Solomon, S., Garcia, R. R., Rowland, F. S., and Wuebbles, D. J.: On the depletion of Antarctic ozone, *Nature*, 321, 755–758, 1986. 2075
- 25 Tabazadeh, A., Turco, R. P., Drdla, K., and Jacobson, M. Z.: A model for studying the composition and chemical effects of stratospheric aerosols, *J. Geophys. Res.*, 99, 12897–12914, 1994. 2073
- Tabazadeh, A., Toon, O. B., and Jensen, E. J.: Formation and implications of ice particle nucleation in the stratosphere, *Geophys. Res. Lett.*, 24, 2007–2010, 1997. 2074, 2075
- 30 Tabazadeh, A., Djikaev, Y. S., Hamill, P., and Reiss, H.: Laboratory evidence for surface nucleation of solid polar stratospheric cloud particles, *J. Phys. Chem.*, 106, 10238–10246, 2002. 2073, 2074
- Tolbert, M. A., Rossi, M. J., Malhotra, R., and Golden, D. M.: Reaction of chlorine nitrate with

**The submodel PSC  
in EMAC**

O. Kirner et al.

[Title Page](#)[Abstract](#)[Introduction](#)[Conclusions](#)[References](#)[Tables](#)[Figures](#)[◀](#)[▶](#)[◀](#)[▶](#)[Back](#)[Close](#)[Full Screen / Esc](#)[Printer-friendly Version](#)[Interactive Discussion](#)

hydrogen-chloride and water at Antarctic stratospheric temperatures, *Science*, 238, 1258–1260, 1987. 2075

Tost, H., Jöckel, P., Kerkweg, A., Sander, R., and Lelieveld, J.: Technical note: A new comprehensive SCAVenging submodel for global atmospheric chemistry modelling, *Atmos. Chem. Phys.*, 6, 565–574, doi:10.5194/acp-6-565-2006, 2006a. 2078

Tost, H., Jöckel, P., and Lelieveld, J.: Influence of different convection parameterisations in a GCM, *Atmos. Chem. Phys.*, 6, 5475–5493, doi:10.5194/acp-6-5475-2006, 2006b. 2078

Tost, H., Jöckel, P., Kerkweg, A., Pozzer, A., Sander, R., and Lelieveld, J.: Global cloud and precipitation chemistry and wet deposition: tropospheric model simulations with ECHAM5/MESSy1, *Atmos. Chem. Phys.*, 7, 2733–2757, doi:10.5194/acp-7-2733-2007, 2007a. 2078

Tost, H., Jöckel, P., and Lelieveld, J.: Lightning and convection parameterisations - uncertainties in global modelling, *Atmos. Chem. Phys.*, 7, 4553–4568, doi:10.5194/acp-7-4553-2007, 2007b. 2078

Turco, R. P., Toon, O. B., and Hamill, P.: Heterogeneous physicochemistry of the polar ozone hole, *J. Geophys. Res.*, 94, 16493–16510, 1989 2090

van den Broek, M. M. P., Williams, J. E., and Bregman, A.: Implementing growth and sedimentation of NAT particles in a global Eulerian model, *Atmos. Chem. Phys.*, 4, 1869–1883, doi:10.5194/acp-4-1869-2004, 2004. 2078, 2083

Waibel, A.: Anomalien ozonchemisch relevanter Spurengase, Dissertation an der Universität Heidelberg, Shaker, Aachen, Germany, 1997. 2092, 2093

Waibel, A. E., Peter, T. H., Carslaw, K. S., Oelhaf, H., Wetzell, G., Crutzen, P. J., Poschl, U., Tsias, A., Reimer, V., and Fischer, H.: Arctic ozone loss due to denitrification, *Science*, 283, 2064–2069, 1999. 2073

Walcek, C. J.: Minor flux adjustment near mixing ratio extremes for simplified yet highly accurate monotonic calculation of tracer advection, *J. Geophys. Res.*, 105, 9335–9348, 2000. 2094

Wirth, M., Tsias, A., Förnbrack, A., Weiß, V., Carslaw, K. S., Leutbecher, M., Renber, W., Volkert, H., and Peter, T.: Model-guided Lagrangian observation and simulation of mountain polar stratospheric clouds, *J. Geophys. Res.*, 104, 23971–23981, 1999. 2073, 2074

Wofsy, S., Salawitch, R., Yatteau, J., McElroy, M., Gandrud, B., Dye, J., and Baumgardner, D.: Condensation of HNO<sub>3</sub> on falling ice particles: Mechanism for denitrification of the polar stratosphere, *Geophys. Res. Lett.*, 17, 449–452, 1990 2074



The submodel PSC  
in EMAC

O. Kirner et al.

**Table 2.** Reaction probabilities  $\gamma$  in the PSC submodel. Not in italics:  $\gamma$  from laboratory studies, valid for the temperature range in parentheses (Sander et al., 2003, 2006). In italics:  $\gamma$  as used in the original code of the “Mainz Stratospheric Box Model” (Carslaw et al., 1994).

Heterogeneous reaction	on ice particles	on NAT particles
(R1) $\text{N}_2\text{O}_5(\text{g}) + \text{H}_2\text{O}(\text{s})$	0.02 (188–195 K)	$4 \times 10^{-4}$ (200 K)
(R2) $\text{N}_2\text{O}_5(\text{g}) + \text{HCl}(\text{s})$	0.03 (190–220 K)	0.003 (200 K)
(R3) $\text{ClONO}_2(\text{g}) + \text{H}_2\text{O}(\text{s})$	0.3 (180–200 K)	0.004 (200–202 K)
(R4) $\text{ClONO}_2(\text{g}) + \text{HCl}(\text{s})$	0.3 (180–200 K)	0.2 (185–210 K)
(R5) $\text{ClONO}_2(\text{g}) + \text{HBr}(\text{s})$	0.3 (200 K)	0.3 (200 K)
(R6) $\text{BrONO}_2(\text{g}) + \text{H}_2\text{O}(\text{s})$	0.3 (190–200 K)	<i>0.001</i>
(R7) $\text{BrONO}_2(\text{g}) + \text{HCl}(\text{s})$	<i>0.3</i>	<i>0.3</i>
(R8) $\text{HOCl}(\text{g}) + \text{HCl}(\text{s})$	0.2 (195–200 K)	0.1 (195–200 K)
(R9) $\text{HOCl}(\text{g}) + \text{HBr}(\text{s})$	0.3 (189 K)	<i>0.3</i>
(R10) $\text{HOBr}(\text{g}) + \text{HCl}(\text{s})$	0.3 (180–228 K)	<i>0.1</i>
(R11) $\text{HOBr}(\text{g}) + \text{HBr}(\text{s})$	0.1 (228 K)	<i>0.1</i>

[Title Page](#)[Abstract](#)[Introduction](#)[Conclusions](#)[References](#)[Tables](#)[Figures](#)[I◀](#)[▶I](#)[◀](#)[▶](#)[Back](#)[Close](#)[Full Screen / Esc](#)[Printer-friendly Version](#)[Interactive Discussion](#)

**Table 3.** The PSC Submodel CTRL and CPL namelists in the namelist file psc.nml, which is part of the MESSy user interface. The settings have been used for the simulation which results are presented in Sect. 5.

<i>&amp;CTRL</i>	
<i>KinPar</i> = T	switch for the kinetic growth NAT parameterisation (True/False)
<i>LAdvectionNat</i> = F	influence of the advection to the formation of ice and NAT (True/False) with <i>KinPar</i> = T → only influence to the formation of ice
<i>LHomNucNAT</i> = F	homogen NAT-nucleation? (True/False) with <i>KinPar</i> = T → irrelevant
<i>NatFormThreshold</i> = -3.0	supercooling for initialisation of NAT in K
<i>minKhet</i> = 0.0	minimal reaction rate for the heterogeneous reactions in $\text{cm}^3 \text{s}^{-1}$
<i>maxKhet</i> = $1.0 \times 10^{-13}$	maximal reaction rate for the heterogeneous reactions in $\text{cm}^3 \text{s}^{-1}$
<i>SupSatIce</i> = 1.5	supercooling in percentage of $\text{H}_2\text{O}$ partial pressure
$r_{\min} = 1.0 \times 10^{-7}$	with <i>KinPar</i> = F → minimal radius of solid particles ( $r_{\text{solid}}$ ) in m with <i>KinPar</i> = T → minimal radius of ice particles ( $r_{\text{ice}}$ ) in m
$N_{\max} = 42\,000$	with <i>KinPar</i> = F → maximal number density of solid particles in particles $\text{m}^{-3}$ with <i>KinPar</i> = T → maximal number density of ice particles in particles $\text{m}^{-3}$
<i>SedScheme</i> = 1	switch for sedimentation schemes: 1 = simple upwind scheme 2 = Walcek advection scheme 3 = trapezoid scheme else = no sedimentation
<i>&amp;CPL</i>	
<i>LCalcChem</i> = F	switch for computation of heterogeneous reaction rates in submodel PSC (True/False)
<i>TempShift</i> = 0.0	internal change of temperature in K in submodel PSC
$r_{\text{lat}} = -55.0, 45.0$	latitude limit of PSC region (SH, NH)
$r_{\text{lb}} = 18000.0, 18000.0$	lower boundary of PSC region [Pa] (SH, NH)
$r_{\text{mb}} = 14000.0, 10000.0$	middle boundary of PSC region [Pa] (SH, NH)
$r_{\text{ub}} = 500.0, 500.0$	upper boundary of PSC region [Pa] (SH, NH)
$l_{\text{feedback}} = T$	feedback on dynamics

## The submodel PSC in EMAC

O. Kirner et al.

Title Page

Abstract

Introduction

Conclusions

References

Tables

Figures

◀

▶

◀

▶

Back

Close

Full Screen / Esc

Printer-friendly Version

Interactive Discussion



## The submodel PSC in EMAC

O. Kirner et al.

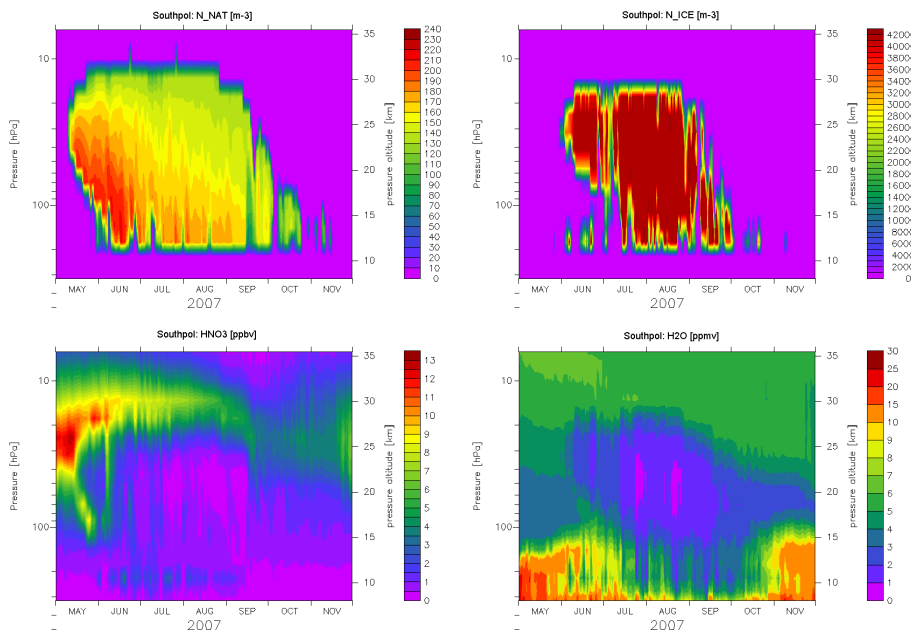


**Fig. 1.** Time series from May 2007 to November 2007 (zonally averaged polewards of 87.9° S): number density of NAT particles ( $N_{\text{NAT}}$  in particles  $\text{m}^{-3}$ , top left), number density of ice particles ( $N_{\text{ICE}}$  in particles  $\text{m}^{-3}$ , top right), mixing ratio of HNO<sub>3</sub> (in  $\text{nmol mol}^{-1}$ , bottom left) and mixing ratio of H<sub>2</sub>O (in  $\mu\text{mol mol}^{-1}$ , bottom right).

Title Page

Abstract

Introduction

Conclusions

References

Tables

Figures

◀

▶

◀

▶

Back

Close

Full Screen / Esc

Printer-friendly Version

Interactive Discussion

